

Constraints on interacting dark energy models from time-delay cosmography with seven lensed quasars

Ling-Feng Wang,¹ Jie-Hao Zhang,¹ Dong-Ze He,² Jing-Fei Zhang¹ and Xin Zhang^{1,3,4*}

¹Department of Physics, College of Sciences, Northeastern University, Shenyang 110819, China

²College of Sciences, Chongqing University of Posts and Telecommunications, Chongqing 400065, China

³Frontiers Science Center for Industrial Intelligence and Systems Optimization, Northeastern University, Shenyang 110819, China

⁴Key Laboratory of Data Analytics and Optimization for Smart Industry (Northeastern University), Ministry of Education, Shenyang 110819, China

Accepted 2022 May 24. Received 2022 May 21; in original form 2021 November 15

ABSTRACT

Measurements of time-delay cosmography of lensed quasars can provide an independent probe to explore the expansion history of the late-time Universe. In this paper, we employ the time-delay cosmography measurements from seven lenses (here abbreviated as the TD data) to constrain interacting dark energy (IDE) models. We mainly focus on the scenario of vacuum energy (with $w = -1$) interacting with cold dark matter, and consider four typical cases of the interaction form Q . When the TD data alone are employed, we find that the IDE models with $Q \propto \rho_{\text{de}}$ seem to have an advantage in relieving the H_0 tension between the cosmic microwave background (CMB) and TD data. When the TD data are added to the CMB+BAO+SN+ H_0 data, we find that: (i) the coupling parameter β in all the considered IDE models is positive within 1σ range, implying a mild preference for the case of cold dark matter decaying into dark energy; (ii) the IDE model with $Q = \beta H_0 \rho_c$ slightly relieves the S_8 tension, but the other considered IDE models further aggravate this tension; (iii) the Akaike information criteria of the IDE models with $Q \propto \rho_c$ are lower than that of the Λ CDM model, indicating that these IDE models are more preferred by the current mainstream data. We conclude that the considered IDE models have their own different advantages when the TD data are employed, and none of them can achieve good scores in all aspects.

Key words: gravitational lensing; strong – quasars: general – cosmological parameters – dark energy – dark matter

1 INTRODUCTION

The precise measurement of the cosmic microwave background (CMB) anisotropies indicates the dawn of an era of precision cosmology (Bennett et al. 2003; Spergel et al. 2003). Six basic parameters in the standard Λ CDM model have been constrained precisely by the *Planck* CMB observation (Aghanim et al. 2020), and the Λ CDM model can excellently fit most of the observational data with the least free parameters. Nevertheless, theoretically, the Λ CDM model suffers from the fine-tuning and cosmic coincidence problems (Weinberg 1989). Furthermore, the Hubble constant H_0 inferred from the *Planck* CMB observation combined with the Λ CDM model (Aghanim et al. 2020) is above 5σ tension with the direct measurements by the SH0ES (Supernovae H0 for the Equation of State) team (Riess et al. 2021) using the distance ladder method (see reviews by e.g. Knox & Millea 2020; Di Valentino et al. 2021a,c; Jedamzik et al. 2021; Perivolaropoulos & Skara 2021; Shah et al. 2021; Abdalla et al. 2022). Thus, some extensions to the Λ CDM model are expected to be necessary not only for the development of cosmological theories, but also for the interpretation of experimental results (Di Valentino et al. 2021c; Abdalla et al. 2022).

Among various extensions to the Λ CDM model, a variety of models based on the scenario of dark energy interacting with cold dark matter, referred to as the interacting dark energy (IDE) models, have

attracted lots of attention (see Wang et al. 2016 for a recent review). This scenario could help resolve the cosmic coincidence problem (e.g. Comelli et al. 2003; Cai & Wang 2005; Zhang 2005; He & Wang 2008; He et al. 2009) and relieve the H_0 tension (e.g. Di Valentino et al. 2017; Yang et al. 2018b,a; Pan et al. 2019; Di Valentino et al. 2020a,b; Vagnozzi 2020; Gao et al. 2021). In addition, the knowledge of dark energy and dark matter is still very scarce, and whether there exists a direct, non-gravitational interaction between them has yet to be verified. Therefore, indirectly detecting the interaction between dark sectors via cosmological observations is one of the important missions in current cosmology (e.g. Guo et al. 2007; Li et al. 2009; Xia 2009; He et al. 2011; Li et al. 2011; Li & Zhang 2011; Fu et al. 2012; Zhang et al. 2012, 2014; Cui et al. 2015; Feng & Zhang 2016; Murgia et al. 2016; Xia & Wang 2016; Costa et al. 2017; Guo et al. 2018; Li et al. 2019; Asghari et al. 2020; Cheng et al. 2020; Feng et al. 2020; Li et al. 2020a; Pan et al. 2020; Aljaf et al. 2021; Carrilho et al. 2021; Di Valentino et al. 2021d; Lucca 2021b; Samart et al. 2021; Yang et al. 2021). Describing the interaction between dark sectors usually requires the introduction of extra parameters in the base Λ CDM model, which cannot be precisely constrained by the CMB data, because these extra parameters are highly degenerate with other cosmological parameters. For the sake of breaking the cosmological parameter degeneracies and constraining the interaction between dark sectors more precisely, a variety of precise late-Universe probes are required (e.g. Yang et al. 2019; Li et al. 2020b; Zhang et al. 2021).

Time-delay cosmography is a promising late-Universe probe, pro-

* E-mail: zhangxin@mail.neu.edu.cn

viding independent measurements for H_0 by measuring the time delays between the multiple images of gravitational lenses (Treu & Marshall 2016). Compared with the distance ladder, this method measures the combination of absolute angular diameter distances rather than relative distances, so it can provide constraints on H_0 . In 1964, Refsdal (1964) proposed that the angular diameter distance of the lens system could be inferred by measuring the arrival time difference Δt for the light rays from different paths. Active galactic nucleus is the background source that can provide a sufficiently variable luminosity to measure the time delay (Vanderriest et al. 1989; Schechter et al. 1997; Fassnacht et al. 1999; Kochanek et al. 2006; Eigenbrod et al. 2006a). In 1979, the first strongly lensed quasar with two images was discovered (Walsh et al. 1979), and the first robust time delays were measured in 1997 (Kundic et al. 1997). Whereafter, time-delay cosmography gradually becomes a high-profile cosmological probe aimed at the late-time Universe (e.g. Fassnacht et al. 2002; Kochanek 2002; Koopmans et al. 2003; Eigenbrod et al. 2006b; Fassnacht et al. 2006; Paraficz & Hjorth 2009; Suyu et al. 2013; Jee et al. 2015; Meng et al. 2015; Bonvin et al. 2016; Chen et al. 2016; Collett & Cunningham 2016; Jee et al. 2016).

Recently, the H0LiCOW (H0 Lenses in COSMOGRAIL’s Well-spring) collaboration employed the time-delay cosmography measurements with six lensed quasars to infer the H_0 value (Wong et al. 2020). The inferred H_0 value in a spatially flat Λ CDM cosmology is $73.3^{+1.7}_{-1.8}$ km s⁻¹ Mpc⁻¹, which is in 3.1σ tension with the *Planck* CMB result. This tension further increases to 5.3σ when combining the time-delay cosmography with the local H_0 measurement by the SH0ES team. Wong et al. (2020) have considered several extended cosmological models to relieve the H_0 tension, and found that the tension still exists in those extended models. Then, the STRIDES (STRong-lensing Insights into Dark Energy Survey) collaboration employed the time-delay cosmography from the single lens DES J0408–5354 to infer the H_0 value, and obtained $H_0 = 74.2^{+2.7}_{-3.0}$ km s⁻¹ Mpc⁻¹ with precision of 3.9% (Shajib et al. 2020), which is in 2.2σ tension with the *Planck* CMB result. Whereafter, the TDCOSMO (Time-Delay COSMOgraphy) collaboration reanalysed the lensed quasars in the H0LiCOW and STRIDES samples to investigate the effect of lens mass models on the systematic uncertainties (Birrer et al. 2020; Millon et al. 2020), and obtained $H_0 = 74.0^{+1.7}_{-1.8}$ km s⁻¹ Mpc⁻¹ (composite model) and $H_0 = 74.2 \pm 1.6$ km s⁻¹ Mpc⁻¹ (power-law model), which are consistent with the previous results. The H_0 tension between the *Planck* CMB observation and the time-delay cosmography reflects the inconsistency of the measurements between the early and late Universe. The IDE models may have the potential to relieve the H_0 tension by introducing the interaction between dark sectors, but a detailed analysis on various IDE models with the time-delay cosmography is lacking so far.

In the light of the introduction above, we find that there are several important questions that deserve to be studied: (i) which type of the IDE models has advantage in relieving the H_0 tension between the time-delay cosmography and the CMB observation; (ii) how the time-delay cosmography affects the cosmological constraints on the interaction between dark energy and cold dark matter; (iii) which type of the IDE models is more favoured by the current mainstream data sets including the time-delay cosmography. To answer these questions, in this paper, we employ the time-delay cosmography measurements from seven lensed quasars to constrain several typical IDE models.

The rest of this paper is organized as follows. In Section 2, we introduce the theoretical basis of the time–delay cosmography and

the IDE models, and show the observational data considered in this work. In Section 3, we report the constraint results and give detailed discussions. Finally, the conclusion is given in Section 4.

2 METHODS AND DATA

2.1 Time-delay cosmography

When a massive object (the lens) lies between a background source and an observer, the background source may be gravitationally lensed into multiple images. The light rays corresponding to different image positions travel through different space-time paths. Since these paths have different gravitational potentials and lengths, these light rays will reach the observer at different times. If the source has flux variations, the time delays between multiple images can be measured by monitoring the lens (Schechter et al. 1997; Fassnacht et al. 1999, 2002; Kochanek et al. 2006; Courbin et al. 2011).

If the foreground lens and the background source are sufficiently aligned, multiple images of the background source may be formed. The light rays observed at different images have different excess time delays when they reach the observer. The excess time delay between two images is defined by

$$\Delta t_{ij} = \frac{D_{\Delta t}}{c} \left[\frac{(\theta_i - \beta)^2}{2} - \psi(\theta_i) - \frac{(\theta_j - \beta)^2}{2} + \psi(\theta_j) \right], \quad (1)$$

where θ_i and θ_j are the positions of images i and j in the image plane, respectively. The lens potentials at the image positions, $\psi(\theta_i)$ and $\psi(\theta_j)$, and the source position β , can be determined from the mass model of the system. The time-delay distance $D_{\Delta t}$ (Refsdal 1964; Suyu et al. 2010) is defined as a combination of three angular diameter distances,

$$D_{\Delta t} \equiv (1 + z_d) \frac{D_d D_s}{D_{ds}}, \quad (2)$$

where z_d is the redshift of the lens, D_d is the angular diameter distance to the lens, D_s is the angular diameter distance to the source, and D_{ds} is the angular diameter distance between the lens and the source. If the time delay Δt_{ij} can be measured and an accurate lens model is available to determine the lens potential $\psi(\theta)$, then the time-delay distance can be determined. By further assuming a cosmological model, $D_{\Delta t}$ can be used to constrain cosmological parameters.

2.2 Interacting dark energy models

In the context of a spatially flat Friedmann–Robertson–Walker universe, the Friedmann equation is written as

$$3M_{\text{pl}}^2 H^2 = \rho_{\text{de}} + \rho_{\text{c}} + \rho_{\text{b}} + \rho_{\text{r}}, \quad (3)$$

where $3M_{\text{pl}}^2 H^2$ is the critical density of the Universe, ρ_{de} , ρ_{c} , ρ_{b} , and ρ_{r} represent the energy densities of dark energy, cold dark matter, baryon, and radiation, respectively.

In the IDE models, the assumption of some direct, non-gravitational interaction between dark energy and cold dark matter is made. Under this assumption, in the level of phenomenological study, the energy conservation equations for dark energy and cold dark matter are given by

$$\dot{\rho}_{\text{de}} + 3H(1+w)\rho_{\text{de}} = Q, \quad (4)$$

$$\dot{\rho}_{\text{c}} + 3H\rho_{\text{c}} = -Q, \quad (5)$$

where the dot denotes the derivative with respect to the cosmic time

Table 1. The TD data from seven lensed quasars, including the measurements of z_d , z_s , and $D_{\Delta t}$. Here, z_s is the redshift of the source.

Lens name	z_d	z_s	$D_{\Delta t}$ (Mpc)
B1608+656 (Suyu et al. 2010; Jee et al. 2019)	0.6304	1.394	5156^{+296}_{-236}
RXJ1131–1231 (Suyu et al. 2014; Chen et al. 2019)	0.295	0.654	2096^{+98}_{-83}
HE 0435–1223 (Wong et al. 2017; Chen et al. 2019)	0.4546	1.693	2707^{+183}_{-168}
SDSS 1206+4332 (Birrer et al. 2019)	0.745	1.789	5769^{+589}_{-471}
WFI2033–4723 (Rusu et al. 2020)	0.6575	1.662	4784^{+399}_{-248}
PG 1115+080 (Chen et al. 2019)	0.311	1.722	1470^{+137}_{-127}
DES J0408–5354 (Agnello et al. 2017; Shajib et al. 2020)	0.597	2.375	3382^{+146}_{-115}

t , w is the equation of state parameter of dark energy, and Q describes the energy transfer rate between dark sectors.

Since the fundamental nature of dark energy is still unclear, it is difficult to understand the microscopic origin of the interaction between dark energy and cold dark matter. Therefore, we can only study the IDE in a pure phenomenological way (e.g. Zhang 2005; Zhang et al. 2008, 2010; Li et al. 2011; Li & Zhang 2014; Zhang et al. 2014; Li et al. 2014a,b; Geng et al. 2015; Li et al. 2016). The form of Q is usually assumed to be proportional to the energy density of dark energy or cold dark matter, or some mixture of the two (e.g. Amendola 1999; Billyard & Coley 2000). The proportionality coefficient Γ has the dimension of energy, and so it is with the form of $\Gamma = \beta H$ or $\Gamma = \beta H_0$, where β is the dimensionless coupling parameter. $\beta = 0$ indicates no interaction between dark energy and cold dark matter, $\beta > 0$ means cold dark matter decaying into dark energy, and $\beta < 0$ means dark energy decaying into cold dark matter.

In this work, we study the minimal version of extension to the base Λ CDM model in the context of IDE. Hence, we consider only the case of $w = -1$, in order not to introduce more extra parameters. If there is no interaction between dark sectors, the case of $w = -1$ corresponds to the vacuum energy, serving as a pure background in the cosmological evolution. However, when there is some interaction between dark sectors, even though we have $w = -1$, the corresponding dark energy cannot serve as a pure background and it actually is not a vacuum energy in essence. Here we do not wish to study the nature of dark energy with a purely theoretical point of view, but instead we wish to study the problem concerning dark energy in a phenomenological way. Thus, we call the dark energy with $w = -1$ vacuum energy for convenience in this paper, and the corresponding IDE model is denoted as the I Λ CDM model. In this work, we take four specific forms of Q as typical examples to make an analysis of the IDE models, i.e., $Q = \beta H_0 \rho_c$ (I Λ CDM1), $Q = \beta H_0 \rho_{de}$ (I Λ CDM2), $Q = \beta H \rho_c$ (I Λ CDM3), and $Q = \beta H \rho_{de}$ (I Λ CDM4).

In the IDE cosmology, the early-time superhorizon cosmological perturbations occasionally diverge (in a part of the parameter space of the model) if the dark energy perturbations are considered, leading to a catastrophe in cosmology as the perturbations enter the horizon. In order to avoid such a cosmological catastrophe caused by the interaction between dark sectors, one has to consider some effective schemes to properly calculate the perturbations of dark energy, instead of using a conventional way of treating dark energy as a perfect fluid with negative pressure. In 2014, Li et al. (2014a,b) extended the parametrized post-Friedmann (PPF) approach (Fang et al. 2008; Hu 2008) to involve the IDE. Such an extended version of PPF method, referred to as ePPF for convenience, can successfully avoid the perturbation divergence problem in the IDE cosmology. In this work, we

consider the I Λ CDM model in which the ‘‘vacuum energy’’ is not a true background due to the interaction, thus we also need to consider its perturbations. Therefore, we employ the ePPF method (Li et al. 2014a,b) to treat the cosmological perturbations in this work (see e.g. Li et al. 2016; Zhang 2017; Feng et al. 2018 for more applications of the ePPF method).

2.3 Observational data

We employ the modified version of the Markov Chain Monte Carlo package COSMOMC (Lewis & Bridle 2002) to infer the posterior distributions of the cosmological parameters. The observational data used in this paper include the CMB data, the baryon acoustic oscillation (BAO) data, the type Ia supernova (SN) data, the H_0 data, the galaxy clustering (GC) and weak lensing (WL) data, and the time-delay cosmography data. Unless otherwise specified, we use the abbreviation ‘TD’ to represent the time-delay cosmography data in the following. The details of these data are listed as follows.

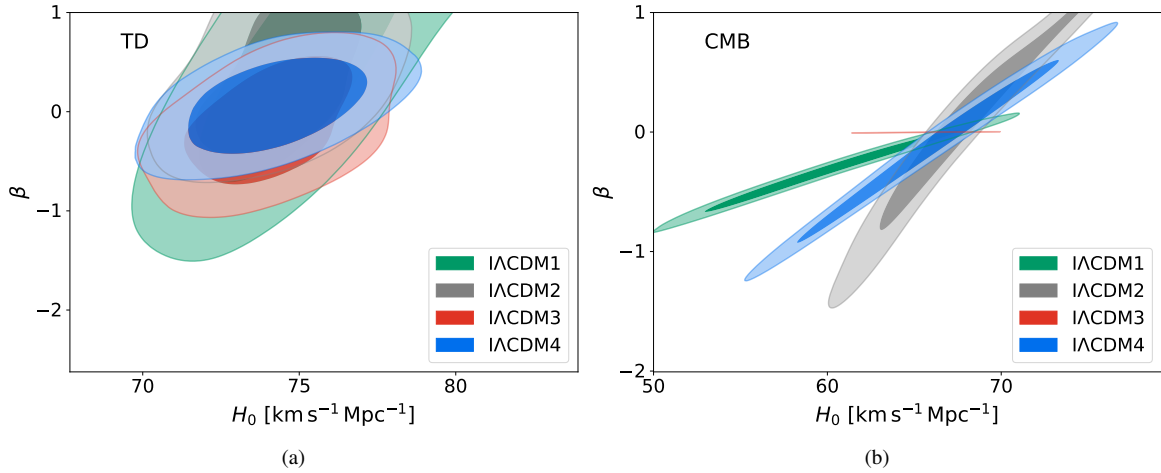
- (i) The CMB data: the *Planck* TT, TE, EE spectra at $\ell \geq 30$, the low- ℓ temperature Commander likelihood, and the low- ℓ SimAll EE likelihood, from the *Planck* 2018 data release (Aghanim et al. 2020).
- (ii) The BAO data: the measurements from 6dFGS ($z_{\text{eff}} = 0.106$) (Beutler et al. 2011), SDSS-MGS ($z_{\text{eff}} = 0.15$) (Ross et al. 2015), and BOSS DR12 ($z_{\text{eff}} = 0.38, 0.51, \text{ and } 0.61$) (Alam et al. 2017).
- (iii) The SN data: the latest Pantheon sample comprised of 1048 data points from the Pantheon compilation (Scolnic et al. 2018).
- (iv) The H_0 data: the measurement result of $H_0 = 74.03 \pm 1.42$ km s $^{-1}$ Mpc $^{-1}$ from distance ladder reported by the SH0ES team (Riess et al. 2019).
- (v) The GC and WL data: the GC and WL data from the first year observation of the Dark Energy Survey (DES; Abbott et al. 2018).
- (vi) The TD data: the measurements of the time-delay cosmography from seven lensed quasars (six HOLiCOW lenses and one STRIDES lens), as listed in Table 1.

3 RESULTS AND DISCUSSIONS

In this section, we report our constraint results in detail, and make some analyses and discussions on them. First, we shall report the constraint results from the TD data alone, and make a comparison for the four types of IDE models in relieving the H_0 tension. Then, we add the local H_0 measurement by the SH0ES team to the TD data, for the sake of further showing the H_0 tension between the CMB and TD+ H_0 data. Thirdly, we employ the CMB+BAO+SN+ H_0 and

Table 2. Fitting results (68.3 per cent confidence level) in the Λ CDM and IDE models from the CMB and TD data. Here, H_0 is in units of $\text{km s}^{-1} \text{Mpc}^{-1}$.

Data	Parameter	Λ CDM	IACDM1	IACDM2	IACDM3	IACDM4
CMB	H_0	67.15 ± 0.61	$60.4^{+4.5}_{-5.3}$	67.3 ± 3.2	65.5 ± 1.8	66.1 ± 4.6
	Ω_m	0.3177 ± 0.0085	$0.51^{+0.11}_{-0.19}$	0.32 ± 0.13	0.341 ± 0.025	0.35 ± 0.15
	β	–	-0.31 ± 0.21	$-0.04^{+0.70}_{-0.44}$	-0.0023 ± 0.0023	$-0.11^{+0.54}_{-0.44}$
TD	H_0	73.8 ± 1.6	74.3 ± 1.9	74.3 ± 1.8	74.1 ± 1.7	74.2 ± 1.8
	Ω_m	$0.249^{+0.022}_{-0.028}$	$0.258^{+0.025}_{-0.017}$	$0.253^{+0.024}_{-0.018}$	$0.263^{+0.013}_{-0.019}$	0.261 ± 0.016
	β	–	> -0.246	$0.21^{+0.50}_{-0.46}$	$-0.11^{+0.50}_{-0.36}$	0.07 ± 0.31
H_0 tension		3.88σ	2.64σ	1.91σ	3.47σ	1.64σ

**Figure 1.** 2D marginalized contours (68.3 and 95.4 per cent confidence levels) in the H_0 – β planes for the IDE models by using the TD and CMB data.

CMB+BAO+SN+ H_0 +TD data to constrain the IDE models, in order to investigate the effect of adding the TD data to the mainstream observational data on the cosmological parameters. In addition, we shall also use the information criterion as a statistical tool to judge how well the IDE models can fit the data. We use the abbreviation ‘CBSH’ to denote the CMB+BAO+SN+ H_0 data.

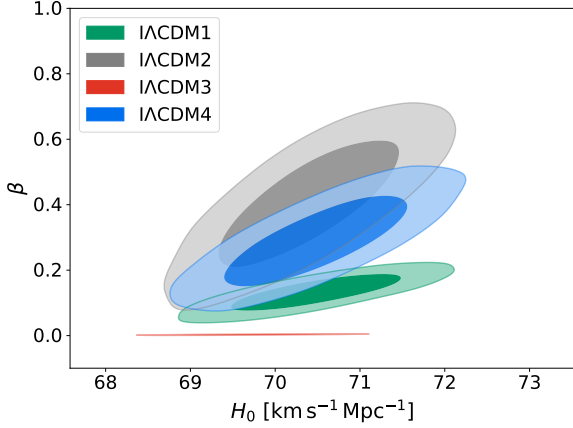
We first report the constraint results from the TD data alone, which are shown in Table 2. For the parameter H_0 , the TD data can constrain it with precision of ~ 2 per cent in the Λ CDM and IDE models. The inferred H_0 value is $73.8 \pm 1.6 \text{ km s}^{-1} \text{Mpc}^{-1}$ in the Λ CDM model, which is in 3.88σ tension with the CMB data. In the four IDE models, the inferred H_0 values are 74.3 ± 1.9 (IACDM1), 74.3 ± 1.8 (IACDM2), 74.1 ± 1.7 (IACDM3), and 74.2 ± 1.8 (IACDM4) $\text{km s}^{-1} \text{Mpc}^{-1}$. The H_0 tensions are relieved to a certain extent in all the IDE models, and especially in the IACDM2 and IACDM4 models, the tensions are reduced to 1.91σ and 1.64σ , respectively. However, these results actually do not support that the IACDM2 and IACDM4 models can relieve the H_0 tension. In fact, the contours in Fig. 1(a) show that there is no significant correlation between the parameters β and H_0 when the TD data are employed, indicating that these IDE models cannot effectively change the H_0 values through introducing an interaction between the dark sectors. From Fig. 1(b) and Table 2 we can see that the reason why the IDE models seem to relieve the H_0 tension is the large errors of H_0 given by the CMB data, but not the better overlaps of parameter spaces. We note that in

the IDE models, the constraints on the parameters are so loose that the posterior distributions obviously fluctuate with repeated analyses. Therefore, we choose the median values of multiple analyses as the final displayed results, and we verify that such an approach would not affect our main conclusions. We also note that when only the CMB data are employed, the constraint results of H_0 in this paper are different from several previous papers (Di Valentino et al. 2020a; Di Valentino 2021; Lucca & Hooper 2020). For example, given the same IDE model (the IACDM model with $Q \propto H\rho_{\text{de}}$), the constraint results of H_0 are $66.1 \pm 4.6 \text{ km s}^{-1} \text{Mpc}^{-1}$ in this paper but $72.8^{+3.0}_{-1.5} \text{ km s}^{-1} \text{Mpc}^{-1}$ in Di Valentino et al. (2020a). This difference is arising from the different treatments for cosmological perturbations. To avoid the perturbation divergence problem existing in the IDE cosmology, the priors of β and w are set to $\beta > 0$ and $w > -1$ (in this case w is fixed to $w = -0.999$) in Di Valentino et al. (2020a), but the ePPF method used in this paper allows us to explore the whole parameter space without assuming any specific priors on w and β .

Then, for the sake of further showing the H_0 tension between the CMB observation and the late-Universe observations, we combine the TD data with the local H_0 measurement by the SH0ES team to give constraints on the IDE models. The constraint results from the TD+ H_0 data are listed in Table 3. Because adding the local H_0 measurement in the data set is just equivalent to putting a prior on H_0 , the constraint errors of H_0 become smaller, but the constraint errors of β are still too large. There is still no significant correlation

Table 3. Fitting results (68.3 per cent confidence level) in the Λ CDM and IDE models from the TD+ H_0 data. Here, H_0 is in units of $\text{km s}^{-1} \text{Mpc}^{-1}$.

Parameter	Λ CDM	IACDM1	IACDM2	IACDM3	IACDM4
H_0	73.9 ± 1.1	74.2 ± 1.2	74.2 ± 1.0	74.1 ± 1.0	74.0 ± 1.1
Ω_m	$0.224^{+0.044}_{-0.033}$	0.262 ± 0.020	$0.260^{+0.013}_{-0.016}$	$0.2603^{+0.0088}_{-0.015}$	$0.261^{+0.015}_{-0.017}$
β	–	> -0.162	$0.24^{+0.37}_{-0.28}$	$0.06^{+0.27}_{-0.22}$	$0.10^{+0.23}_{-0.30}$
H_0 tension	5.37σ	2.74σ	2.06σ	4.18σ	1.67σ


Figure 2. 2D marginalized contours (68.3 and 95.4 per cent confidence levels) in the H_0 - β plane for the IDE models by using the CBSH+TD data.

between the parameters β and H_0 , similar to the case of using the TD data alone. Specifically, the H_0 value is $73.9 \pm 1.1 \text{ km s}^{-1} \text{Mpc}^{-1}$ in the Λ CDM model, which is in 5.37σ tension with the value inferred from the CMB data. In the four IDE models, the H_0 value are 74.2 ± 1.2 (IACDM1), 74.2 ± 1.0 (IACDM2), 74.1 ± 1.0 (IACDM3), and 74.0 ± 1.1 (IACDM4) $\text{km s}^{-1} \text{Mpc}^{-1}$. Compared with the 5.37σ tension in the Λ CDM model, the H_0 tensions are reduced to 2.06σ and 1.67σ in the IACDM2 and IACDM4 model, respectively. As discussed above, these reductions of H_0 tensions are actually due to the large errors of H_0 from the CMB data, but not the better overlaps of parameter spaces.

As for the coupling parameter β , the TD data alone cannot constrain it well. The TD data are actually the combination of the angular diameter distance that is inversely proportional to H_0 , and thus the TD data are more sensitive to H_0 than to β . Therefore, we have to combine the TD data with the current mainstream observations, i.e., the CMB, BAO, SN, and H_0 data, to constrain the coupling parameter β . Although in principle there is an inconsistency between the TD data and the CMB data in constraining H_0 , we still give the joint constraints for completeness of the analysis. Here, we consider the local H_0 measurement reported by the SH0ES team as a prior and add it to the CMB+BAO+SN data. It should be added that a more reasonable approach to combine the SN and H_0 data is to adopt the local prior of SN Ia absolute magnitude instead of the corresponding prior of H_0 , which can avoid double counting of low-redshift supernovae (e.g. Camarena & Marra 2020a,b, 2021).

When using the CBSH data without the TD data, the constraint values of the β values are 0.095 ± 0.040 (IACDM1), 0.33 ± 0.14 (IACDM2), 0.0021 ± 0.0011 (IACDM3), and 0.225 ± 0.093 (IACDM4). In all the four IDE models, the β values are positive,

corresponding to the case of cold dark matter decaying into dark energy. In IACDM3, the value of β is close to zero, meaning that the CBSH data support no interaction between dark energy and cold dark matter in this model. When using the CBSH+TD data, the β values are 0.132 ± 0.037 (IACDM1), 0.41 ± 0.13 (IACDM2), 0.0031 ± 0.0011 (IACDM3), and 0.293 ± 0.092 (IACDM4). It is shown that, when the TD data are added, the errors of β are only slightly reduced, because the TD data cannot constrain β tightly. The central values of β become higher, because β and H_0 are positively correlated and adding the TD data makes the H_0 values higher, which can be seen from Fig. 2. Higher positive values of β further support the scenario that cold dark matter decays into dark energy.

Now, we give a discussion on the parameter S_8 , defined as $S_8 \equiv \sigma_8 \sqrt{\Omega_m/0.3}$, with σ_8 being the amplitude of mass fluctuations. The GC and WL data from DES give the results of $S_8 = 0.773^{+0.026}_{-0.020}$ (DES Year 1) (Abbott et al. 2018) and $S_8 = 0.776^{+0.017}_{-0.017}$ (DES Year 3) (Abbott et al. 2022), which are in more than 2σ tension with $S_8 = 0.834^{+0.016}_{-0.016}$ inferred from the *Planck* CMB data (Aghanim et al. 2020). In previous works (e.g. Di Valentino et al. 2020a,b, 2021b; Gao et al. 2021; Lucca 2021a,b; Abdalla et al. 2022; de Araujo et al. 2021), the IDE models are considered to relieve the S_8 tension. We also wish to investigate the effect of the TD data on S_8 in this work. However, the TD data alone cannot provide direct constraints on the parameter S_8 , due to the fact that the time-delay distance provides only the geometrical information of the Universe, while constraining S_8 needs the information of the large-scale structure. Even so, when combined with other observational data, the TD data may indirectly affect the constraints on S_8 through constraining other cosmological parameters. Therefore, we discuss the effect of the TD data on S_8 in the context of the CBSH and CBSH+TD data. Since the S_8 values inferred from the DES Year 1 and DES Year 3 data have no obvious difference; in this paper, we employ only the DES Year 1 data for the cosmological analysis and leave the DES Year 3 data for future works.

When the GC and WL data are employed, the inferred S_8 values are $0.772^{+0.019}_{-0.021}$ (Λ CDM), $0.760^{+0.034}_{-0.030}$ (IACDM1), $0.785^{+0.048}_{-0.064}$ (IACDM2), 0.771 ± 0.026 (IACDM3), and $0.786^{+0.054}_{-0.069}$ (IACDM4). We calculate the S_8 tensions by comparing these inferred S_8 values with the CBSH and CBSH+TD results reported in Table 4. When the CBSH data are employed, the S_8 tensions in the IACDM1, IACDM3, and IACDM4 models are 1.38σ , 1.47σ , and 1.34σ , respectively, slightly relieved compared with 1.59σ in the Λ CDM model. When the CBSH+TD data are employed, compared with the Λ CDM model, almost all the considered IDE models further aggravate the S_8 tension, except the IACDM1 model very slightly relieving the tension from 1.16σ to 1.11σ . The slight alleviation of the S_8 tension is due to the fact that S_8 is determined by both σ_8 and Ω_m . Although higher H_0 leads to higher σ_8 , Ω_m becomes lower at the same time, as shown

Table 4. Fitting results (68.3 per cent confidence level) in the Λ CDM and IDE models from the CBSH and CBSH+TD data. Here, H_0 is in units of $\text{km s}^{-1} \text{Mpc}^{-1}$.

Data	Parameter	Λ CDM	IACDM1	IACDM2	IACDM3	IACDM4
CBSH	H_0	68.20 ± 0.42	69.57 ± 0.73	69.58 ± 0.75	68.96 ± 0.60	69.65 ± 0.74
	Ω_m	0.3034 ± 0.0055	0.274 ± 0.013	0.230 ± 0.032	0.2950 ± 0.0071	0.241 ± 0.026
	β	–	0.095 ± 0.040	0.33 ± 0.14	0.0021 ± 0.0011	0.225 ± 0.093
	σ_8	0.8049 ± 0.0072	0.845 ± 0.018	$1.047^{+0.088}_{-0.160}$	0.820 ± 0.011	$0.990^{+0.072}_{-0.110}$
	S_8	0.809 ± 0.012	0.807 ± 0.012	$0.906^{+0.038}_{-0.060}$	0.813 ± 0.012	$0.882^{+0.031}_{-0.042}$
	S_8 tension	1.59σ	1.38σ	1.63σ	1.47σ	1.34σ
	χ^2_{\min}	3825.487	3822.547	3825.248	3825.206	3825.253
	ΔAIC	0	–0.940	1.760	1.719	1.765
CBSH+TD	H_0	68.67 ± 0.41	70.48 ± 0.67	70.40 ± 0.71	69.72 ± 0.56	70.50 ± 0.71
	Ω_m	0.2975 ± 0.0053	0.259 ± 0.011	0.205 ± 0.031	0.2862 ± 0.0064	0.217 ± 0.026
	β	–	0.132 ± 0.037	0.41 ± 0.13	0.0031 ± 0.0011	0.293 ± 0.092
	σ_8	0.8026 ± 0.0073	0.858 ± 0.018	$1.14^{+0.10}_{-0.19}$	0.826 ± 0.011	$1.072^{+0.079}_{-0.140}$
	S_8	0.799 ± 0.012	0.798 ± 0.012	$0.932^{+0.043}_{-0.069}$	0.807 ± 0.012	$0.904^{+0.034}_{-0.050}$
	S_8 tension	1.16σ	1.11σ	1.86σ	1.26σ	1.58σ
	χ^2_{\min}	3844.530	3835.107	3843.417	3840.304	3844.153
	ΔAIC	0	–7.423	0.887	–2.226	1.622

in Fig. 3(a) and 3(b). These two opposite effects eventually make S_8 become lower, as shown in Fig. 3(c).

Finally, we compare the IDE models on the basis of their fittings to the observational data. It is unfair to use only χ^2_{\min} to judge how well the models can fit the data, because the IDE models have one more free parameter (β) than the Λ CDM model. Hence, we use the Akaike information criterion (AIC; Szydlowski et al. 2015), defined as $\text{AIC} \equiv \chi^2_{\min} + 2d$, with d being the number of free parameters, to compare the fittings. In order to show the differences of AIC values between the Λ CDM and IDE models more clearly, we set the AIC value of the Λ CDM model to be zero, and list the values of $\Delta \text{AIC} = \Delta \chi^2 + 2\Delta d$ in Table 4, with $\Delta \chi^2 = \chi^2_{\min, \text{IDE}} - \chi^2_{\min, \Lambda \text{CDM}}$ and $\Delta d = d_{\text{IDE}} - d_{\Lambda \text{CDM}} = 1$. A model with a lower value of AIC is more supported by the observational data.

When the CBSH data are employed to constrain the IDE models, the ΔAIC values of the IDE models are –0.940 (IACDM1), 1.760 (IACDM2), 1.719 (IACDM3), and 1.765 (IACDM4). Only the IACDM1 model has a slightly lower AIC than the Λ CDM model. The absolute values of ΔAIC in all the four IDE models are not large, indicating that the CBSH data support the IDE and Λ CDM models to the similar extent. However, this situation changes significantly when the TD data are added. When we use the CBSH+TD data, the ΔAIC values of the IACDM1 and IACDM3 models dramatically decrease, with $\Delta \text{AIC} = -7.423$ (IACDM1) and $\Delta \text{AIC} = -2.226$ (IACDM3). This indicates that the data sets including the TD data support the IDE models with $Q \propto \rho_c$ more than those with $Q \propto \rho_{\text{de}}$. Especially for the IACDM1 model ($Q = \beta H_0 \rho_c$), its AIC value is significantly lower than that of the Λ CDM model. We can conclude that this model has more advantages than the Λ CDM model, in terms of fitting the observational data.

4 CONCLUSIONS

Time-delay cosmography provides an important complement to the late-Universe observations, based on the time-delay effect of strong gravitational lensing, coding the information of the time-delay distance $D_{\Delta t}$ defined as a combination of angular diameter distances. In this work, we investigate the implications of the time-delay cosmography on the IDE models. The measurements of time-delay cosmography from seven lensed quasars, abbreviated as the TD data, are considered. Four representative IDE models, i.e., the IACDM1 ($Q = \beta H_0 \rho_c$), IACDM2 ($Q = \beta H_0 \rho_{\text{de}}$), IACDM3 ($Q = \beta H \rho_c$), and IACDM4 ($Q = \beta H \rho_{\text{de}}$) models, are considered in this work. We first employ the TD data alone to constrain the IDE models, and then we combine the TD data with the local H_0 measurement by the SH0ES team to address the H_0 tension. Then we combine the TD data with the CMB+BAO+SN+ H_0 data to give constraints on the coupling parameter β , and discuss the S_8 tension. Finally, we discuss the comparison of the IDE models according to the fitting results. The main findings from our analyses are summarized as follows.

(i) When the TD data alone are employed, the H_0 tensions between the CMB and TD data are reduced from 3.88σ (Λ CDM) to 1.91σ (IACDM2) and 1.64σ (IACDM4), respectively. When combining the TD data and the local H_0 measurement by the SH0ES team, the H_0 tensions are reduced from 5.37σ (Λ CDM) to 2.06σ (IACDM2) and 1.67σ (IACDM4). This implies that the IDE models with the interaction term $Q \propto \rho_{\text{de}}$ seem to have an advantage in relieving the H_0 tension between the CMB and TD data. However, it is hard to draw a firm conclusion, because the reductions of the H_0 tensions are mainly due to the relatively large errors of H_0 inferred from the CMB data in the IDE models.

(ii) The TD data alone cannot constrain the coupling parameter β well. Adding the TD data to the CBSH data, the central values of β increase due to the positive correlation between the param-

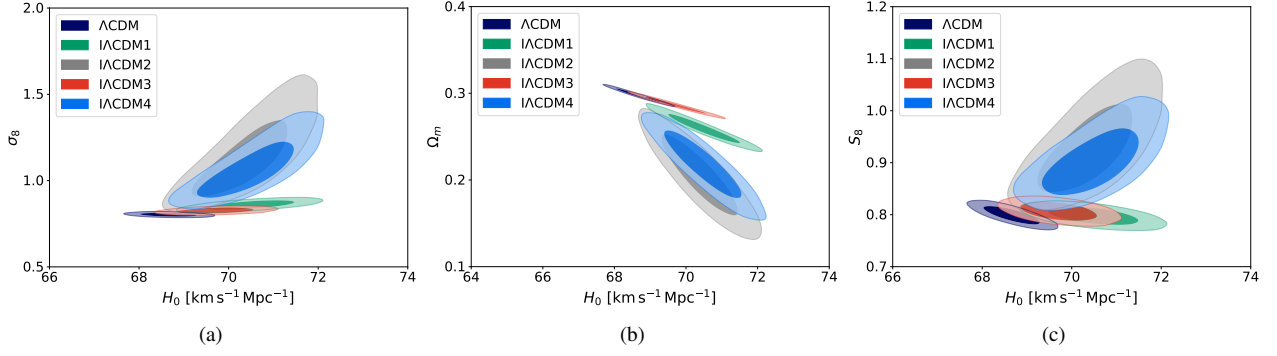


Figure 3. 2D marginalized contours (68.3 and 95.4 per cent confidence levels) in the H_0 – σ_8 , H_0 – Ω_m , and H_0 – S_8 planes for the Λ CDM model and the IDE models by using the CBSH+TD data.

ters β and H_0 . The β values are 0.132 ± 0.037 (IACDM1), 0.41 ± 0.13 (IACDM2), 0.0031 ± 0.0011 (IACDM3), and 0.293 ± 0.092 (IACDM4) when the CBSH+TD data are employed. The β values are positive within 1σ range in the four IDE models, corresponding to the case of cold dark matter decaying into dark energy.

(iii) When the CBSH+TD data are employed, only the IACDM1 model can relieve the S_8 tension very slightly, while the other IDE models further aggravate the S_8 tension. This indicates that the IDE models have no obvious advantage in relieving the S_8 tension, although the IDE model with $Q = \beta H_0 \rho_c$ shows a mild advantage.

(iv) When the CBSH data are employed, the Δ AIC values of the IDE models are not very different, but when the TD data are added, the Δ AIC values of the IACDM1 and IACDM3 model are obviously lower than the other IDE models, especially for the IACDM1 model ($Q = \beta H_0 \rho_c$) with Δ AIC = -7.423 . From the perspective of fitting the observational data, the IDE model with $Q = \beta H_0 \rho_c$ is more supported by the CBSH+TD data than the Λ CDM model.

In summary, the IDE models with $Q \propto \rho_{de}$ seem to have an advantage in relieving the H_0 tension between the early-Universe and late-Universe measurements; all the considered IDE models have no obvious advantage in relieving the S_8 tension; the IDE models with $Q \propto \rho_c$ have advantages in fitting the observational data. None of the considered IDE models can perform well in all aspects. The performance of more potential IDE models in the TD data will be studied in our future work. In the future, more TD data will be obtained, helping us use late-Universe cosmological probes to further study the interaction between dark energy and dark matter.

ACKNOWLEDGEMENTS

This work was supported by the National Natural Science Foundation of China (grant numbers 11975072, 11835009, 11875102, and 11690021), the Liaoning Revitalization Talents Program (grant number XLYC1905011), the Fundamental Research Funds for the Central Universities (grant number N2005030), the National Program for Support of Top-Notch Young Professionals (grant number W02070050), the National 111 Project of China (grant number B16009), and the Science Research Grants from the China Manned Space Project (grant number CMS-CSST-2021-B01).

DATA AVAILABILITY

The data underlying this article will be shared on reasonable request to the corresponding author.

REFERENCES

- Abbott T. M. C., et al., 2018, *Phys. Rev. D*, 98, 043526
 Abbott T. M. C., et al., 2022, *Phys. Rev. D*, 105, 023520
 Abdalla E., et al., 2022, *J. High Energy Astrophys.*, 34, 49
 Aghanim N., et al., 2020, *A&A*, 641, A6
 Agnello A., et al., 2017, *MNRAS*, 472, 4038
 Alam S., et al., 2017, *MNRAS*, 470, 2617
 Aljaf M., Gregoris D., Khurshudyan M., 2021, *Eur. Phys. J. C*, 81, 544
 Amendola L., 1999, *Phys. Rev. D*, 60, 043501
 Asghari M., Khosravi S., Mollazadeh A., 2020, *Phys. Rev. D*, 101, 043503
 Bennett C., et al., 2003, *ApJS*, 148, 1
 Beutler F., et al., 2011, *MNRAS*, 416, 3017
 Billyard A. P., Coley A. A., 2000, *Phys. Rev. D*, 61, 083503
 Birrer S., et al., 2019, *MNRAS*, 484, 4726
 Birrer S., et al., 2020, *A&A*, 643, A165
 Bonvin V., Tewes M., Courbin F., Kuntzer T., Sluse D., Meylan G., 2016, *A&A*, 585, A88
 Cai R.-G., Wang A., 2005, *J. Cosmol. Astropart. Phys.*, 2005, 002
 Camarena D., Marra V., 2020a, *Phys. Rev. Res.*, 2, 013028
 Camarena D., Marra V., 2020b, *MNRAS*, 495, 2630
 Camarena D., Marra V., 2021, *MNRAS*, 504, 5164
 Carrilho P., Moretti C., Bose B., Markovič K., Pourtsidou A., 2021, *J. Cosmol. Astropart. Phys.*, 2021, 004
 Chen G. C. F., et al., 2016, *MNRAS*, 462, 3457
 Chen G. C.-F., et al., 2019, *MNRAS*, 490, 1743
 Cheng G., Ma Y.-Z., Wu F., Zhang J., Chen X., 2020, *Phys. Rev. D*, 102, 043517
 Collett T. E., Cunnington S. D., 2016, *MNRAS*, 462, 3255
 Comelli D., Pietroni M., Riotto A., 2003, *Phys. Lett. B*, 571, 115
 Costa A. A., Xu X.-D., Wang B., Abdalla E., 2017, *J. Cosmol. Astropart. Phys.*, 2017, 028
 Courbin F., et al., 2011, *A&A*, 536, A53
 Cui J.-L., Yin L., Wang L.-F., Li Y.-H., Zhang X., 2015, *J. Cosmol. Astropart. Phys.*, 2015, 024
 Di Valentino E., 2021, *MNRAS*, 502, 2065
 Di Valentino E., Melchiorri A., Mena O., 2017, *Phys. Rev. D*, 96, 043503
 Di Valentino E., Melchiorri A., Mena O., Vagnozzi S., 2020a, *Phys. Dark Univ.*, 30, 100666
 Di Valentino E., Melchiorri A., Mena O., Vagnozzi S., 2020b, *Phys. Rev. D*, 101, 063502
 Di Valentino E., et al., 2021a, *Class. Quantum. Gravity*, 38, 153001
 Di Valentino E., et al., 2021b, *Astropart. Phys.*, 131, 102604

- Di Valentino E., et al., 2021c, *Astropart. Phys.*, 131, 102605
- Di Valentino E., Melchiorri A., Mena O., Pan S., Yang W., 2021d, *MNRAS*, 502, L23
- Eigenbrod A., Courbin F., Dye S., Meylan G., Sluse D., Saha P., Vuissoz C., Magain P., 2006a, *A&A*, 451, 747
- Eigenbrod A., Courbin F., Meylan G., Vuissoz C., Magain P., 2006b, *A&A*, 451, 759
- Fang W., Hu W., Lewis A., 2008, *Phys. Rev. D*, 78, 087303
- Fassnacht C., Pearson T., Readhead A., Browne I., Koopmans L., Myers S., Wilkinson P., 1999, *ApJ*, 527, 498
- Fassnacht C., Xanthopoulos E., Koopmans L., Rusin D., 2002, *ApJ*, 581, 823
- Fassnacht C. D., Gal R. R., Lubin L. M., McKean J. P., Squires G. K., Readhead A. C. S., 2006, *ApJ*, 642, 30
- Feng L., Zhang X., 2016, *J. Cosmol. Astropart. Phys.*, 2016, 072
- Feng L., Li Y.-H., Yu F., Zhang J.-F., Zhang X., 2018, *Eur. Phys. J. C*, 78, 865
- Feng L., He D.-Z., Li H.-L., Zhang J.-F., Zhang X., 2020, *Sci. China Phys. Mech. Astron.*, 63, 290404
- Fu T.-F., Zhang J.-F., Chen J.-Q., Zhang X., 2012, *Eur. Phys. J. C*, 72, 1932
- Gao L.-Y., Zhao Z.-W., Xue S.-S., Zhang X., 2021, *J. Cosmol. Astropart. Phys.*, 2021, 005
- Geng J.-J., Li Y.-H., Zhang J.-F., Zhang X., 2015, *Eur. Phys. J. C*, 75, 356
- Guo Z.-K., Ohta N., Tsujikawa S., 2007, *Phys. Rev. D*, 76, 023508
- Guo R.-Y., Zhang J.-F., Zhang X., 2018, *Chin. Phys. C*, 42, 095103
- He J.-H., Wang B., 2008, *J. Cosmol. Astropart. Phys.*, 2008, 010
- He J.-H., Wang B., Zhang P., 2009, *Phys. Rev. D*, 80, 063530
- He J.-H., Wang B., Abdalla E., 2011, *Phys. Rev. D*, 83, 063515
- Hu W., 2008, *Phys. Rev. D*, 77, 103524
- Jedamzik K., Pogosian L., Zhao G.-B., 2021, *Commun. in Phys.*, 4, 123
- Jee I., Komatsu E., Suyu S. H., 2015, *J. Cosmol. Astropart. Phys.*, 2015, 033
- Jee I., Komatsu E., Suyu S. H., Huterer D., 2016, *J. Cosmol. Astropart. Phys.*, 2016, 031
- Jee I., Suyu S., Komatsu E., Fassnacht C. D., Hilbert S., Koopmans L. V., 2019, *Science*, 365, 1134
- Knox L., Millea M., 2020, *Phys. Rev. D*, 101, 043533
- Kochanek C. S., 2002, *ApJ*, 578, 25
- Kochanek C. S., Morgan N., Falco E., McLeod B., Winn J., Dembicky J., Ketzbeck B., 2006, *ApJ*, 640, 47
- Koopmans L. V. E., Treu T., Fassnacht C. D., Blandford R. D., Surpi G., 2003, *ApJ*, 599, 70
- Kundic T., et al., 1997, *ApJ*, 482, 75
- Lewis A., Bridle S., 2002, *Phys. Rev. D*, 66, 103511
- Li Y.-H., Zhang X., 2011, *Eur. Phys. J. C*, 71, 1700
- Li Y.-H., Zhang X., 2014, *Phys. Rev. D*, 89, 083009
- Li M., Li X.-D., Wang S., Wang Y., Zhang X., 2009, *J. Cosmol. Astropart. Phys.*, 2009, 014
- Li Y., Ma J., Cui J., Wang Z., Zhang X., 2011, *Sci. China Phys. Mech. Astron.*, 54, 1367
- Li Y.-H., Zhang J.-F., Zhang X., 2014a, *Phys. Rev. D*, 90, 063005
- Li Y.-H., Zhang J.-F., Zhang X., 2014b, *Phys. Rev. D*, 90, 123007
- Li Y.-H., Zhang J.-F., Zhang X., 2016, *Phys. Rev. D*, 93, 023002
- Li H.-L., Feng L., Zhang J.-F., Zhang X., 2019, *Sci. China Phys. Mech. Astron.*, 62, 120411
- Li H.-L., Zhang J.-F., Zhang X., 2020a, *Commun. Theor. Phys.*, 72, 125401
- Li H.-L., He D.-Z., Zhang J.-F., Zhang X., 2020b, *J. Cosmol. Astropart. Phys.*, 2020, 038
- Lucca M., 2021a, *Phys. Dark Univ.*, 34, 100899
- Lucca M., 2021b, *Phys. Rev. D*, 104, 083510
- Lucca M., Hooper D. C., 2020, *Phys. Rev. D*, 102, 123502
- Meng X.-L., Treu T., Agnello A., Auger M. W., Liao K., Marshall P. J., 2015, *J. Cosmol. Astropart. Phys.*, 2015, 059
- Millon M., et al., 2020, *A&A*, 639, A101
- Murgia R., Gariazzo S., Fornengo N., 2016, *J. Cosmol. Astropart. Phys.*, 2016, 014
- Pan S., Yang W., Di Valentino E., Saridakis E. N., Chakraborty S., 2019, *Phys. Rev. D*, 100, 103520
- Pan S., de Haro J., Yang W., Amorós J., 2020, *Phys. Rev. D*, 101, 123506
- Paraficz D., Hjorth J., 2009, *A&A*, 507, L49
- Perivolaropoulos L., Skara F., 2021, preprint (arXiv:2105.05208)
- Refsdal S., 1964, *MNRAS*, 128, 307
- Riess A. G., Casertano S., Yuan W., Macri L. M., Scolnic D., 2019, *ApJ*, 876, 85
- Riess A. G., et al., 2021, preprint (arXiv:2112.04510)
- Ross A. J., Samushia L., Howlett C., Percival W. J., Burden A., Manera M., 2015, *MNRAS*, 449, 835
- Rusu C. E., et al., 2020, *MNRAS*, 498, 1440
- Samart D., Silasan B., Channuie P., 2021, *Phys. Rev. D*, 104, 063517
- Schechter P. L., et al., 1997, *ApJ*, 475, L85
- Scolnic D. M., et al., 2018, *ApJ*, 859, 101
- Shah P., Lemos P., Lahav O., 2021, *A&AR*, 29, 9
- Shajib A. J., et al., 2020, *MNRAS*, 494, 6072
- Spergel D., et al., 2003, *ApJS*, 148, 175
- Suyu S., Marshall P., Auger M., Hilbert S., Blandford R., Koopmans L., Fassnacht C., Treu T., 2010, *ApJ*, 711, 201
- Suyu S. H., et al., 2013, *ApJ*, 766, 70
- Suyu S., et al., 2014, *ApJ*, 788, L35
- Szydlowski M., Krawiec A., Kurek A., Kamionka M., 2015, *Eur. Phys. J. C*, 75, 5
- Treu T., Marshall P. J., 2016, *A&AR*, 24, 11
- Vagnozzi S., 2020, *Phys. Rev. D*, 102, 023518
- Vanderriest C., Schneider J., Herpe G., Chevreton M., Moles M., Wlerick G., 1989, *A&A*, 215, 1
- Walsh D., Carswell R. F., Weymann R. J., 1979, *Nature*, 279, 381
- Wang B., Abdalla E., Atrio-Barandela F., Pavon D., 2016, *Rept. Prog. Phys.*, 79, 096901
- Weinberg S., 1989, *Rev. Mod. Phys.*, 61, 1
- Wong K. C., et al., 2017, *MNRAS*, 465, 4895
- Wong K. C., et al., 2020, *MNRAS*, 498, 1420
- Xia J.-Q., 2009, *Phys. Rev. D*, 80, 103514
- Xia D.-M., Wang S., 2016, *MNRAS*, 463, 952
- Yang W., Mukherjee A., Di Valentino E., Pan S., 2018a, *Phys. Rev. D*, 98, 123527
- Yang W., Pan S., Di Valentino E., Nunes R. C., Vagnozzi S., Mota D. F., 2018b, *J. Cosmol. Astropart. Phys.*, 2018, 019
- Yang W., Vagnozzi S., Di Valentino E., Nunes R. C., Pan S., Mota D. F., 2019, *J. Cosmol. Astropart. Phys.*, 2019, 037
- Yang W., Pan S., Di Valentino E., Mena O., Melchiorri A., 2021, *J. Cosmol. Astropart. Phys.*, 2021, 008
- Zhang X., 2005, *Mod. Phys. Lett. A*, 20, 2575
- Zhang X., 2017, *Sci. China Phys. Mech. Astron.*, 60, 050431
- Zhang J., Liu H., Zhang X., 2008, *Phys. Lett. B*, 659, 26
- Zhang L., Cui J., Zhang J., Zhang X., 2010, *Int. J. Mod. Phys. D*, 19, 21
- Zhang Z., Li S., Li X.-D., Zhang X., Li M., 2012, *J. Cosmol. Astropart. Phys.*, 2012, 009
- Zhang J., Zhao L., Zhang X., 2014, *Sci. China Phys. Mech. Astron.*, 57, 387
- Zhang M., Wang B., Wu P.-J., Qi J.-Z., Xu Y., Zhang J.-F., Zhang X., 2021, *ApJ*, 918, 56
- de Araujo J. C. N., De Felice A., Kumar S., Nunes R. C., 2021, *Phys. Rev. D*, 104, 104057

This paper has been typeset from a $\text{\TeX}/\text{\LaTeX}$ file prepared by the author.